J Mater Sci (2009) 44:3861–3866
DOI 10.1007/s10853-009-3523-7

Effects of additional elements (M) on the thermal stability and structure of $(Zr_{52.2}Cu_{39.1}Al_{8.7})_{100-x}M_x$ (M = Ag, Be, Gd, x = 8, 7, 2) amorphous alloys

Yong Xu · Yanli Wang · Xiongjun Liu · Guoliang Chen · Yong Zhang

Received: 19 February 2009 / Accepted: 25 April 2009 / Published online: 15 May 2009

Abstract The effects of Ag (8 at.%), Be (7 at.%), and Gd (2 at.%) addition on structure and thermal stability, as well as bulk glass forming ability, in $(Zr_{52.2}Cu_{39.1}Al_{8.7})_{100-x}M_x$ (M = Ag, Be, Gd) alloys are investigated by means of X-ray diffraction and differential scanning calorimetry. The alloy containing Ag and Be have a critical diameter of more than 10 mm, with larger supercooled liquid region and atomic packing efficiency than $Zr_{52.2}Cu_{39.1}Al_{8.7}$ alloy, while the $(Zr_{52.2}Cu_{39.1}Al_{8.7})_{98}Gd_2$ alloy only has a critical diameter of up to 5 mm and shows smaller supercooled liquid region and atomic packing density. CuZr is the main competing crystal phase with amorphous phase in the present Zr-Cu-based alloys. Ag and Be atoms in $Zr_{52.2}Cu_{39.1}Al_{8.7}$ alloy decrease the long range diffusion of Cu atoms and hinder the crystallization process under rapid solidification conditions. As a result, the glass forming ability of $(Zr_{52.2}Cu_{39.1}Al_{8.7})_{92}Ag_8$ and $(Zr_{52.2}Cu_{39.1}Al_{8.7})_{93}Be_7$ alloys are effectively enhanced.

Introduction

Multicomponent bulk metallic glasses have been developed in a number of alloy systems and attracted considerable attention due to their unique properties and promising applications [1–4]. The Zr–Cu binary alloy system exhibits deep eutectics and the fabrication of Φ2 mm fully amorphous rods was recently reported for the binary $Cu_{100-x}Zr_x$ compositions with x = 36 and 50 at.% [5]. The addition of Al can decrease the ternary eutectic melting temperature and strongly enhance the formation of glassy phase in Zr–Cu–Al alloy system [6, 7]. Al substitution in these systems also results in an increased stability of the supercooled liquid [8]. The minor addition of the fourth element, such as Ti, Ni, Ag, Be, and Y, can extremely increase the glass forming ability (GFA) of Zr–Cu–Al alloys. Several Zr–Cu-based bulk metallic glasses, such as Zr–Al–Cu–Ni [9], Zr–Cu–Ti–Ni–Be [10, 11], Zr–Cu–Ti(Nb)–Ni–Al [12], Zr–Cu–Ag–Al [6, 13–16], and Zr–Cu–Pd–Al [17], have been discovered. These alloys have excellent glass forming ability and high thermal stability. For this reason, this group of materials is of significant interest from the views of both fundamental research and industrial applications [8]. In this study, the thermodynamics, kinetics, and structure of $(Zr_{52.2}Cu_{39.1}Al_{8.7})_{100-x}M_x$ (M = Ag, Be, Gd) quaternary alloys have been investigated to analyze the bulk glass forming ability of these alloys.

Experimental

Pre-alloyed $(Zr_{52.2}Cu_{39.1}Al_{8.7})_{100-x}M_x$ (M = Ag, Be, Gd) ingots were prepared by arc melting the mixture of Zr, Cu, Al, Be, Ag, and Gd elements with purity of 99.9% in titanium-gettered argon atmosphere. The alloy ingots with different nominal compositions were obtained: $Zr_{57.1}Cu_{42.9}$, $Zr_{52.2}Cu_{39.1}Al_{8.7}$, $(Zr_{52.2}Cu_{39.1}Al_{8.7})_{92}Ag_8$, $(Zr_{52.2}Cu_{39.1}Al_{8.7})_{93}Be_7$, and $(Zr_{52.2}Cu_{39.1}Al_{8.7})_{98}Gd_2$. The ingots were re-melted several times to obtain master alloys with chemical homogeneity. The alloy rods were prepared, with diameters of 3, 5, 8, and 10 mm, respectively, by using copper mold suction casting. X-ray diffraction (XRD) for phase identification was carried out on a Philips ADP-10

Y. Xu (✉) · Y. Wang · X. Liu · G. Chen · Y. Zhang
State Key Laboratory for Advanced Metals and Materials, University of Science and Technology Beijing, Beijing 100083, China
e-mail: xuyong2612@gmail.com

diffractometer with Mo $K\alpha$ radiation ($\lambda = 0.07093$ nm). The thermal stability associated with glass transition, supercooled liquid region, and crystallization was examined by differential scanning calorimetry (DSC) (TA SDT Q600) at a heating rate of 30 K/min. The density of as-cast alloy was measured by drainage method on Mettler Toledo XS105 DualRange analytical balance (weight resolution of 0.01 mg) at room temperature.

Results

According to the equilibrium phase diagram of Zr–Cu alloy [18], there are six intermediate compounds in Zr–Cu binary system, i.e., Cu_9Zr_2, Cu_8Zr_3, $Cu_{51}Zr_{14}$, $Cu_{10}Zr_7$ ($oC68$), CuZr ($cP2$), and $CuZr_2$ ($tI6$), CuZr stably exists in a temperature range between 988 K and 1208 K and decomposes into $Cu_{10}Zr_7$ and $CuZr_2$ below 988 K [19]. Under equilibrium conditions, the $Zr_{57.1}Cu_{42.9}$ alloy firstly solidifies into Cu_5Zr_8 + CuZr phases, and then the two phases decompose into $CuZr_2$ + $Cu_{10}Zr_7$ phases due to eutectoid reaction at low temperature. However, the experimental cooling conditions usually are not liable to meet the equilibrium solidification conditions, so the phases formed after solidification in the present experiment differ from those formed in the equilibrium process.

When the alloys are slowly-cooled in the furnace, as the master alloy specimens, different phases can be obtained. The main phases in $Zr_{52.2}Cu_{39.1}Al_{8.7}$ alloy are CuZr and $CuZr_2$, as indicated in Fig. 1a. Similarly, the main phases in $(Zr_{52.2}Cu_{39.1}Al_{8.7})_{100-x}M_x$ (M = Ag, Be, Gd) alloys are also CuZr and $CuZr_2$, as indicated in the corresponding XRD patterns shown in Fig. 1b, c, d. As for the addition of Ag (8 at.%) and Be (7 at.%), a broad peak appears at 17° (2θ), indicating the formation of amorphous phase in the alloys. For $(Zr_{52.2}Cu_{39.1}Al_{8.7})_{92}Ag_8$ alloy, the CuZr and $CuZr_2$ peaks are depressed synchronously. However, for $(Zr_{52.2}Cu_{39.1}Al_{8.7})_{98}Gd_2$ alloy, the $CuZr_2$ peaks are extremely enhanced, comparing with $Zr_{52.2}Cu_{39.1}Al_{8.7}$ alloy. The diffraction peaks of the CuZr phase in $(Zr_{52.2}Cu_{39.1}Al_{8.7})_{100-x}M_x$ (M = Ag, Be, Gd) alloys shift slightly to lower or higher angle compared with those in $Zr_{52.2}Cu_{39.1}Al_{8.7}$ alloy because of the distortion of the crystal lattice.

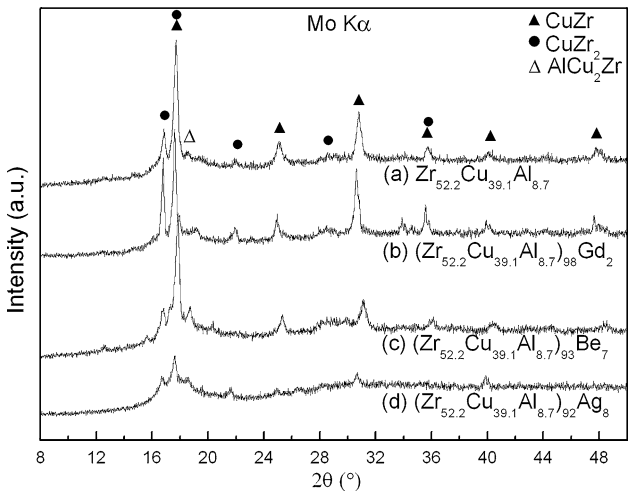

Fig. 1 X-ray diffraction patterns of $Zr_{52.2}Cu_{39.1}Al_{8.7}$ and $(Zr_{52.2}Cu_{39.1}Al_{8.7})_{100-x}M_x$ (M = Ag, Be, Gd) master alloys

When the alloys are rapidly quenched into the cylindrical copper mold with diameter of 3 mm, 5 mm, 8 mm, and 10 mm, respectively, parts of specimens of certain diameter can obtain fully amorphous structure. For $Zr_{52.2}Cu_{39.1}Al_{8.7}$ alloy, CuZr becomes the primary phase with increasing cooling rate and finally disappears in the sample with $d = 3$ mm, as shown in Fig. 2a. As for $(Zr_{52.2}Cu_{39.1}Al_{8.7})_{92}Ag_8$ and $(Zr_{52.2}Cu_{39.1}Al_{8.7})_{93}Be_7$ alloys, the fully bulk metallic glass specimens up to 10 mm diameter can be successfully obtained by an injection mold casting method, as indicated by the corresponding XRD patterns in Fig. 2b, c. The critical diameter of $(Zr_{52.2}Cu_{39.1}Al_{8.7})_{98}Gd_2$ alloy is up to 5 mm. Similar to $Zr_{52.2}Cu_{39.1}Al_{8.7}$ alloy, the main crystal phases in $(Zr_{52.2}Cu_{39.1}Al_{8.7})_{98}Gd_2$ alloy are CuZr and $CuZr_2$ phases, as shown in Fig. 2d.

Figure 3 shows DSC curves obtained from $Zr_{52.2}Cu_{39.1}Al_{8.7}$ and $(Zr_{52.2}Cu_{39.1}Al_{8.7})_{100-x}M_x$ (M = Ag, Be, Gd) glassy alloys. The corresponding parameters, such as glass transition temperature (T_g), temperature of crystallization onset (T_x) and liquidus temperature (T_l), marked by arrows in the DSC curves, are also listed in Table 1.

Thermodynamically, the glass forming ability of the $(Zr_{52.2}Cu_{39.1}Al_{8.7})_{100-x}M_x$ (M = Ag, Be, Gd) alloys can be assessed by the following three parameters: (1) the supercooled liquid region, $\Delta T_x = T_x - T_g$ [20]; (2) the reduced glass transition temperature, $T_{rg} = T_g/T_l$ [21]; and (3) the parameter, $\gamma = T_x/(T_g + T_l)$, which is obtained by simple additive assumption of devitrification tendency of a glass and suppression of crystallization during solidification [22]. As is shown in Table 1, the addition of Ag and Be strongly enlarge supercooled liquid region from 97 K to 113 K for $(Zr_{52.2}Cu_{39.1}Al_{8.7})_{92}Ag_8$ and to 134 K for $(Zr_{52.2}Cu_{39.1}Al_{8.7})_{93}Be_7$, respectively. Meanwhile, due to the addition of Ag and Be, the liquids temperature reduces from 1197 K to 1171 K for $(Zr_{52.2}Cu_{39.1}Al_{8.7})_{92}Ag_8$, and to 1158 K for $(Zr_{52.2}Cu_{39.1}Al_{8.7})_{93}Be_7$, with an enhancement of T_{rg} and γ. In contrast, the addition of Gd (2 at.%) simultaneously decreases T_g, T_x, ΔT_x, T_{rg}, and γ, while increases the liquidus temperature to 1206 K.

As is shown in Table 1, the addition of Ag has little effect on atomic number density of $Zr_{52.2}Cu_{39.1}Al_{8.7}$ alloy. However, the addition of Be increases the atomic number density from 55.7 nm^{-3} to 57.0 nm^{-3} for $(Zr_{52.2}Cu_{39.1}Al_{8.7})_{93}Be_7$, while Gd decreases it to 53.3 nm^{-3}. Not consistent with

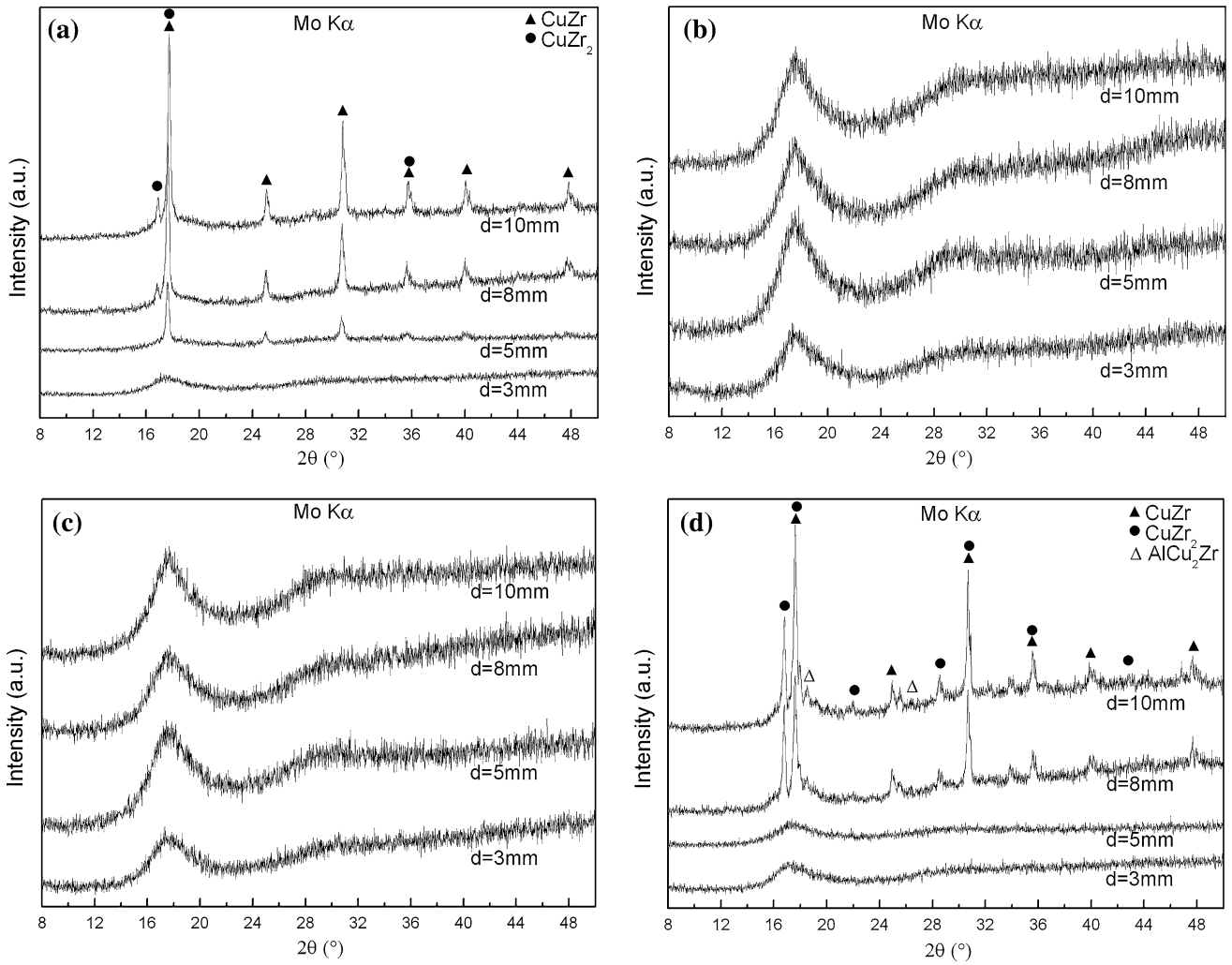

Fig. 2 X-ray diffraction patterns of as-cast: **a** $Zr_{52.2}Cu_{39.1}Al_{8.7}$, **b** $(Zr_{52.2}Cu_{39.1}Al_{8.7})_{92}Ag_8$, **c** $(Zr_{52.2}Cu_{39.1}Al_{8.7})_{93}Be_7$, and **d** $(Zr_{52.2}Cu_{39.1}Al_{8.7})_{98}Gd_2$ alloys

their effects on the atomic number density, the additions of Gd, especially Ag and Be, all improve the GFA of Zr–Cu–Al alloy in our study. The relationship between atomic number density and GFA needs further study to disclose the nature of different influence by the fourth elements.

Discussion

In this study, Be, Ag, and Gd elements are selected owing to their atomic size and negative heat of mixing with Zr or Cu elements. Glass forming ability is a result of the competition between cooling rate and crystallization kinetics, which is closely related to structural, thermodynamic, and kinetic characteristics [16].

The empirical component rules drawn from experimental results [2] have demonstrated that certain atomic-size mismatch and efficient atomic packing enhance the GFA of multicomponent systems. In these $(Zr_{52.2}Cu_{39.1}Al_{8.7})_{100-x}M_x$ (M = Ag, Be, Gd) alloys, atomic radius of each elements is Zr 0.160 nm, Cu 0.128 nm, Al 0.143 nm, Be 0.113 nm, Ag 0.145 nm, and Gd 0.180 nm [23]. The ratio of radii is $r_{Zr/Cu} = 1.25$, $r_{Zr/Al} = 1.12$, $r_{Al/Cu} = 1.12$, $r_{Cu/Be} = 1.13$, $r_{Zr/Ag} = 1.11$, $r_{Ag/Cu} = 1.13$, and $r_{Gd/Zr} = 1.12$, respectively. Therefore, the addition of the fourth element causes more sequential change on atomic-size mismatch, as well as the generation of new atomic pairs (Zr–M, Cu–M, and Al–M). As a result, an efficiently packed local structure will produce, which is often associated with low internal energy and high viscosity of liquid [24]. Heat of mixing values between elements of $(Zr_{52.2}Cu_{39.1}Al_{8.7})_{100-x}M_x$ (M = Ag, Be, Gd) alloys are: Zr–Cu −23 kJ mol^{-1}, Zr–Al −44 kJ mol^{-1}, Zr–Be −43 kJ mol^{-1}, Zr–Ag −20 kJ mol^{-1}, and Cu–Gd −22 kJ mol^{-1} [25, 26]. These large negative values of the heat of mixing can enhance the interactions among the components and promote chemical

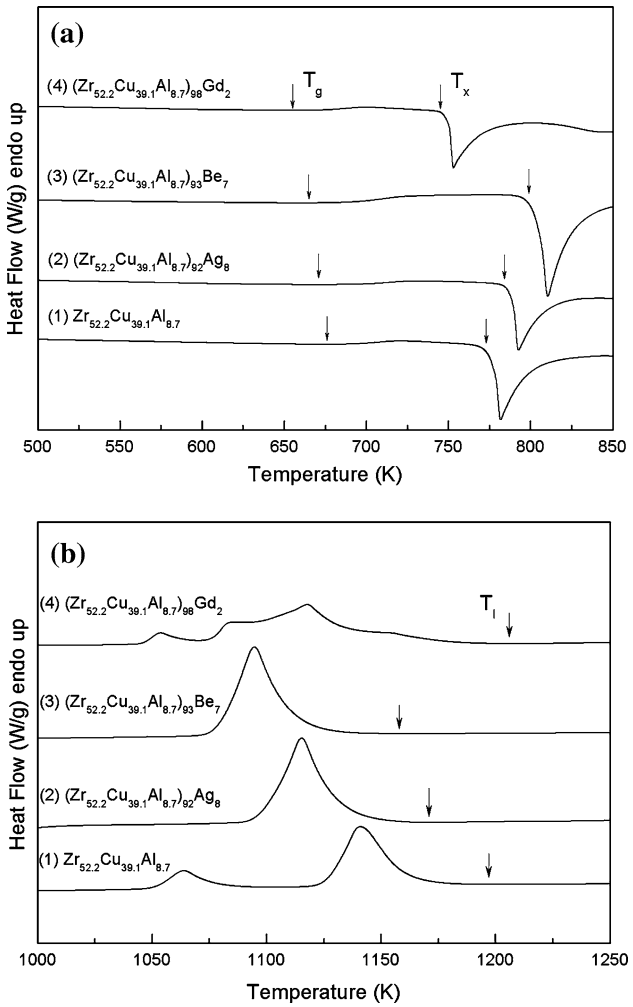

Fig. 3 DSC curves of Zr–Cu–Al and Zr–Cu–Al–M (M = Ag, Be, Gd) glassy alloys with diameter of 1 mm

short range ordering in liquids [24], which can improve local packing efficiency and restrain long range diffusion of atoms [2].

For $(Zr_{52.2}Cu_{39.1}Al_{8.7})_{92}Ag_8$ alloy, the addition of Ag atoms extremely enhances the GFA of $Zr_{52.2}Cu_{39.1}Al_{8.7}$ alloy. From the view of structure, the existence of Ag atoms can hinder the formation of Zr–Cu and Zr–Al pairs in supercooled liquid and avoid the long range diffusion of Cu atoms during the following casting process. Meanwhile, when Ag replace Cu in $CuZr_2$ and CuZr phases, the distortion will be introduced in crystal structure and bring difficulty to crystallization, especially for the more stable $CuZr_2$ phase. The large Ag atoms may lead to more distortion in the body-centered tetragonal lattice of $CuZr_2$ than in the body-centered cubic lattice of CuZr. As a result, the formation of crystal phase is hindered and, on the other side, the formation of amorphous phase is improved.

For $(Zr_{52.2}Cu_{39.1}Al_{8.7})_{93}Be_7$ alloy, its XRD pattern is similar to that of $Zr_{52.2}Cu_{39.1}Al_{8.7}$ alloy under the slow solidification condition, as shown in Fig. 1a, c. It suggests that the addition of Be atoms can partially replace Cu atoms in crystal phases without changing their structure type with low cooling rate. It is thought that Be atoms have larger diffusion coefficient than other atoms and may distribute homogeneously in $(Zr_{52.2}Cu_{39.1}Al_{8.7})_{93}Be_7$ liquid [15], forming the local clusters with larger atomic packing density. When the $(Zr_{52.2}Cu_{39.1}Al_{8.7})_{93}Be_7$ alloy is quenched into the cylindrical copper mold, the homogeneously distributed Be atoms substitute Cu atoms in clusters, which, similar to Ag addition, will introduce great distortion into the local structure. Moreover, considering its smaller atomic size than Ag atoms, Be would bring more instability for the crystal phases than Ag atoms. For this reason, the long range atomic rearrangement, as well as the nucleation and growth rate, can be extremely depressed during casting process, which may improve the stability of supercooled liquid.

For $(Zr_{52.2}Cu_{39.1}Al_{8.7})_{98}Gd_2$ alloy, the addition of Gd decreases the atomic packing density, as well as the thermodynamic parameters of $(Zr_{52.2}Cu_{39.1}Al_{8.7})_{98}Gd_2$ alloy, as shown in Table 1, which may be the negative factors for GFA enhancing. In fact, however, the contribution of Gd atoms to the enhancement of GFA is mainly related to its ability to remove oxygen from the system through preferential formation of gadolinium oxide [27]. It is generally accepted that oxygen is critically detrimental to bulk metallic glass formation, as it can trigger heterogeneous nucleation of various crystal phases. In Zr–Cu-based alloys, oxygen will react with primary elements to form oxides, which may further induce crystallization to form crystal phases [16], such as CuZr, $Cu_{10}Zr_7$, and $CuZr_2$. From the view of thermodynamic, the formation heat of the Gd_2O_3 is about −1827 kJ/mol [28], which is lower than that of the oxides of other constituent elements in Zr–Cu–

Table 1 Summary of the thermal parameters, number density and critical specimen diameter of alloys

Alloy composition (at.%)	T_g (K)	T_x (K)	T_l (K)	ΔT_x (K)	T_{rg}	γ	ρ_0 (nm^{-3})	d_c (mm)
$Zr_{52.2}Cu_{39.1}Al_{8.7}$	676	773	1197	97	0.565	0.413	55.7	3
$(Zr_{52.2}Cu_{39.1}Al_{8.7})_{92}Ag_8$	671	784	1171	113	0.573	0.426	55.7	>10
$(Zr_{52.2}Cu_{39.1}Al_{8.7})_{93}Be_7$	665	799	1158	134	0.574	0.438	57.0	>10
$(Zr_{52.2}Cu_{39.1}Al_{8.7})_{98}Gd_2$	655	745	1206	90	0.543	0.400	53.3	5

Al–Gd alloy (e.g., ZrO_2, −1099 kJ/mol; CuO_2, −167.4 kJ/mol; Al_2O_3, −1670 kJ/mol [28]). Therefore, gadolinium oxides are more favorable to form than the other oxides and a small amount of Gd addition may act as sinks to absorb the oxygen impurity during the repeated re-melting and casting progress [27], which can enhance the GFA of Zr–Cu–Al–Gd alloy. Scavenging effects from some rare-earth elements that alleviate the harmful effect of oxygen have also been observed in other bulk metallic glass systems, such as Mg- and Fe-based alloys [29, 30]. From the view of structure, the addition of Gd in Zr–Cu–Al alloy increases the atomic-size ratio of the constituent elements, which increases the atomic mismatches and the interaction between small and large atoms. Due to its large atomic size, Gd has small diffusion coefficient than other elements, so it will hinder the diffusion of Cu atoms during rapid solidification. Based on the Hume–Rothery rules [27], the solubility of the large atom in crystal phases is likely to be restricted. However, Gd atoms have to redistribute due to its limited solubility in the crystal phases as soon as the crystallization progress begins. The addition of large atoms also makes it difficult to simultaneously satisfy the composition required by crystalline nucleus because more kinds of atoms are involved in the long range rearrangement. These contributions all suppress the formation and growth of the crystal phases and then enhance the GFA.

The diffusion coefficient of Cu is the key factor for improving the GFA of Zr–Cu-based alloys. When the long range diffusion of Cu atoms is depressed, the crystal growth rate will be greatly decreased. The equilibrium solubility of Al in CuZr and $CuZr_2$ intermetallic compound phases is very limited. Therefore, the increase of the concentration of Al in CuZr and $CuZr_2$ phases is attributed to kinetic effects. The interface diffusion coefficient of Al is very small in the Zr–Cu–Al melt when the cooling rate is increased [31]. As a result, the crystal growth rate in the supercooled Zr–Cu–Al alloy is greatly decreased. The fourth element addition in Zr–Cu–Al alloy, such as Ag, Be, or Gd, will effectively depress the formation of crystal phases. In supercooled liquid of $(Zr_{52.2}Cu_{39.1}Al_{8.7})_{100-x}M_x$ (M = Ag, Be, Gd) alloy, the local atomic structure may tend to form clusters consisting of Zr–Ag, Zr–Be, or Cu–Gd atomic pairs, which may decrease the crystal growth rate as the consequence of the 'confusion principle' [32]. During the rapid solidification, Al and M (M = Ag, Be, Gd) atoms do not show a long range redistribution at the solid-liquid interface but are trapped in CuZr and $CuZr_2$ phases, forming the supersaturated intermetallic phases. In comparison with the CuZr and $CuZr_2$ phases, these supersaturated phases have low nucleation rate and crystal growth rate due to their low driving force (free energy difference between the supercooled liquid and the crystal phases) and some kinetic effects (e.g., diffusion rate and interfacial energy). From the above analysis, it can be concluded that the diffusion coefficient of Cu in the supercooled $(Zr_{52.2}Cu_{39.1}Al_{8.7})_{100-x}M_x$ (M = Ag, Be, Gd) melt is much lower than that in the supercooled $Zr_{52.2}Cu_{39.1}Al_{8.7}$ melt, thus the crystal growth rate in the supercooled $Zr_{52.2}Cu_{39.1}Al_{8.7}$ alloy is decreased. And thus the glass forming ability of $(Zr_{52.2}Cu_{39.1}Al_{8.7})_{100-x}M_x$ (M = Ag, Be, Gd) alloy is enhanced.

Conclusions

1. The glass forming ability of $Zr_{52.2}Cu_{39.1}Al_{8.7}$ alloy, as well as the atomic packing density, is greatly increased by the addition of Ag, Be, or Gd atoms, especially for Be addition. The $(Zr_{52.2}Cu_{39.1}Al_{8.7})_{93}Be_7$ alloy has the largest supercooled liquid region up to 134 K. The glassy alloy rods are formed in the diameter range of up to 10 mm for the $(Zr_{52.2}Cu_{39.1}Al_{8.7})_{92}Ag_8$ and $(Zr_{52.2}Cu_{39.1}Al_{8.7})_{93}Be_7$ alloys, and 5 mm for the $(Zr_{52.2}Cu_{39.1}Al_{8.7})_{98}Gd_2$ alloy.
2. CuZr phase is the main competing crystal phase with amorphous phase in these present Zr–Cu-based alloys. The diffusion of Cu atoms could significantly affect the GFA of $(Zr_{52.2}Cu_{39.1}Al_{8.7})_{100-x}M_x$ (M = Ag, Be, Gd) alloys. The fourth element addition decreases the crystal growth rate by depressing the long range diffusion of Cu atoms and thus enhances the GFA.
3. The addition of Ag, Be, or Gd can form Zr–Ag, Zr–Be, or Cu–Gd atomic pairs in supercooled liquid and hinder the formation of Zr–Cu atomic pairs, which introduces large resistance to nucleation and crystallization during rapid solidification.

Acknowledgements This work was financially supported by the National Natural Science Foundation of China (Grants Nos. 50431030, 50471097), National Basic Research Program of China (2007CB613901) and the Program of Introducing Talents of Discipline to Universities (Project No. B07003).

References

1. Johnson WL (1999) MRS Bull (USA) 24:42
2. Inoue A (2000) Acta Mater 48:279
3. El-Hadek MA, Kassem M (2009) J Mater Sci 44:1127. doi:10.1007/s10853-008-3194-9
4. Sharma SK, Strunskus T, Ladebusch H et al (2008) J Mater Sci 43:5495. doi:10.1007/s10853-008-2834-4
5. Xu DH, Lohwongwatana B, Duan G et al (2004) Acta Mater 52:2621
6. Sung DS, Kwon OJ, Fleury E et al (2004) Metal Mater Int 10:575
7. Sun YF, Todaka Y, Umemoto M et al (2008) J Mater Sci 43:7457. doi:10.1007/s10853-008-2634-x
8. Antonowicz J, Louzguine-Luzgin DV, Yavari AR et al (2008) J Alloys Compd. doi:10.1016/j.jallcom.2008.03.092

9. Inoue A, Shibata T, Zhang T (1995) Mater Trans, JIM 36:1420
10. Peker A, Johnson WL (1993) Appl Phys Lett 63:2342
11. Wang G, Jackson I, Fitz Gerald JD et al (2008) J Non-Cryst Solids 354:1575
12. Lin XH, Johnson WL, Rhim WK (1997) Mater Trans, JIM 38:473
13. Inoue A, Zhang W (2003) Appl Phys Lett 83:2351
14. Oh JC, Ohkubo T, Kim YC et al (2005) Scr Mater 53:165
15. Kim YC, Lee JC, Cha PR et al (2006) Mater Sci Eng A 437:248
16. Jiang QK, Wang XD, Nie XP et al (2008) Acta Mater 56:1785
17. Zhang PN, Li JF, Hu Y et al (2008) J Mater Sci 43:7179. doi: 10.1007/s10853-008-3019-x
18. Okamoto H (2008) J Phase Equilib Diffus 29:204
19. He XC, Wang YM, Liu HS et al (2007) J Alloys Compd 439:176
20. Inoue A, Zhang T, Masumoto T (1993) J Non-Cryst Solids 156:473
21. Lu ZP, Tan H, Li Y et al (2000) Scr Mater 42:667
22. Lu ZP, Liu CT (2003) Phys Rev Lett 91:115505
23. Senkov ON, Miracle DB (2001) Mater Res Bull 36:2183
24. Zhang W, Zhang Q, Qin C et al (2008) Mater Sci Eng B 148:92
25. de Boer FR, Boom R, Matterns WCM et al (1988) Cohesion in metals. North-Holland Physics Publishing, Amsterdam
26. Takeuchi A, Inoue A (2005) Mater Trans, JIM 46:2817
27. Fu HM, Wang H, Zhang HF et al (2006) Scr Mater 55:147
28. Pankratz LB, Mrazek RV (1982) Thermodynamic properties of elements and oxides. Department of the Interior, Bureau of Mines, Washington
29. Wei YX, Xi XK, Zhao DQ et al (2005) Mater Lett 59:945
30. Lu ZP, Liu CT, Porter WD (2003) Appl Phys Lett 83:2581
31. Xing LQ, Ochin P (1997) Acta Mater 45:3765
32. Greer AL (1993) Nature 366:303